Case Studies in Thermal Engineering 28 (2021) 101545

Contents lists available at ScienceDirect

Case Studies in Thermal Engineering

journal homepage: www.elsevier.com/locate/csite

Energetic, exergetic and environmental (3E) analyses of different cooling technologies (wet, dry and hybrid) in a CSP thermal power plant

C.G. Cutillas [a], J. Ruiz [a,*], F. Asfand [b], K. Patchigolla [c], M. Lucas [a]

[a] Departamento de Ingeniería Mecánica y Energía, Universidad Miguel Hernández, Avda. de la Universidad, s/n, 03202, Elche, Spain
[b] School of Computing & Engineering, University of Huddersfield, Huddersfield, West Yorkshire, HD1 3DH, UK
[c] Centre for Thermal Energy Systems and Materials, Cranfield University, Bedfordshire, MK43 0AL, UK

ARTICLE INFO

Keywords:
Solar thermal power plant
Condenser
Hybrid system
Exergy
Water consumption

ABSTRACT

This paper deals with the comparison of three condensation systems for the heat dissipation in a solar power plant: wet system, dry system and hybrid system based on the pre-cooling of the air in an adiabatic panel located in the entrance section of a dry system. Energy, exergy and environmental (3E) analyses were conducted to assess the influence of the condensation system on the power plant performance. The Andasol I plant located in Granada (Spain), with a net power capacity of 50 MWe, is used as a real reference case of a concentrated solar power station. The cycle refrigerated with a cooling tower achieves a lower pressure of condensation, followed by the hybrid and dry system. As the pressure decreases, the efficiency of the cycle increases and also the power generated, being 12.60% in the case of cooling tower and 4.65% in the hybrid system with respect the dry condenser. A 71.74% of water usage savings by the hybrid system carries a 7.06% of net power production with regard of the cooling tower configuration. The exergetic performance of the plant is 73.77% for the wet system, 69.21% for the hybrid and 68.46% for the dry system.

1. Introduction

The implementation of renewable energies in our society becomes more and more necessary and thus meets the challenges of clean energy, climate change and sustainable development. The European Strategic Energy Technology Plan states that Concentrated Solar Power/Solar Thermal Electricity (CSP/STE) can make a significant contribution to the transformation of the global energy system by providing an important share of renewable electricity on demand (i.e. flexible electricity dispatch) thanks to the incorporation of in-built storage in CSP/STE plants – which avoids additional grid integration costs. Moreover, by providing flexibility for grid services, CSP/STE can facilitate the integration of variable output renewables such as PV or wind into electricity systems, thereby contributing to the reliability of the transmission grid. The current development of CSP/STE technology has allowed their integration in electricity production systems. A prime example is Spain, where 2.3% of the overall power installed and close to 1.7% of annual electrical energy consumption coming from CSP plants in 2018, Spanish Electricity System report [1]. Although, these data are modest, it is expected that their presence is becoming more relevant around the world. According to the International Energy Agency (IEA) forecasts,

* Corresponding author.
E-mail address: j.ruiz@umh.es (J. Ruiz).

https://doi.org/10.1016/j.csite.2021.101545
Received 20 July 2021; Received in revised form 20 September 2021; Accepted 6 October 2021
Available online 8 October 2021

Nomenclature

C_c	Cycles of concentration (−)
c_p	Specific heat (kJ kg C^{-1})
D	Drift (%)
ex	Specific exergy (kJ kg^{-1})
E	Energy (kJ)
Ex	Exergy (kJ)
$\dot{E}x_d$	Exergy destruction (kW)
g	Gravity (m kg s^{-2})
h	Entalpy (kJ kg^{-1})
h_{s_w}	Enthalpy of saturated air at water temperature, (kJ kg^{-1})
h_v	Enthalpy of vaporization (kJ kg^{-1})
$\dot{m}$	Mass flow (kg s^{-1})
M	Molecular weight (kg $kmol^{-1}$)
Me	Merkel number
p	Pressure (bar)
$\dot{Q}$	Heat rate (kW)
R_a	Dry air gas constant ($R_a = \overline{R}/M_a$)
R_v	Water vapour gas constant ($R_v = \overline{R}/M_v$)
s	Specific entropy (kJ $kg^{-1}K^{-1}$)
T	Temperature (°C)
V	Velocity (m s^{-1})
v	Specific volume (m^3 kg^{-1})
$\dot{W}$	Power (kW)
w_{s_w}	Humidity ratio of saturated air at water temperature
x	Steam quality
x_v^0	Mole fraction of the water vapour
y_D	Exergy destruction rate to total rate of exergy supplied to the system ratio (%)
y_{D_k}	Component exergy destruction rate to total rate of exergy destruction ratio (%)
z	Height (m)

Greek symbols

α	Evaporative pad constant
β	Evaporative pad constant
δ	Thickness of the pad (m)
ε	Exergy efficiency (%)
η	Energy efficiency (%)
ϵ	Evaporation
ω	Specific humidity (kg kg^{-1})
$\widetilde{\omega}$	Humidity ratio parameter ($\widetilde{\omega} = 1.6078\omega$)

Subscripts

0	Dead state
1 to 31	cycle status
amb	Ambient
a to f	bleds
a	Air
b	Blowdown losses
cond	Condenser
cv	Control volume
d	Drift losses
evap	Evaporation losses
f	Saturated liquid
g	Saturated vapour
gross	Gross
i	Inlet
in	Internal
j	j^{th} component
net	Net

yo	Outlet
p	Pump
w	Water
wb	Wet bulb

Abbreviations

ACC	Air cooled condensers
CFH	Closed feedwater heater
CSP	Concentrated solar power
CT	Cooling tower
DCA	Drain cooler approach
HP	High pressure
HRSG	Heat recovery Stem Generator
IP	Intermediate pressure
ITD	Initial Temperature Difference
Le	Lewis number
LP	Low pressure
PV	Photovoltaic
STE	Solar thermal electricity
TTD	Terminal temperature difference

CSP/STE has a huge potential in the long term, ranging from the 357 TWh by 2040 up to 4350 TWh by 2050 according to the hi-Ren scenario (Energy Technology Perspectives 2014), meaning CSP/STE will account for 11% of the electricity generated worldwide and 4% in Europe. The designs of CSP/STE plants are diverse in terms of concentrating technologies (parabolic trough collector (PTC), linear Fresnel, power tower and dish/engine), thermal fluids used and the presence of storage or not. This makes it appealing to CSP designers as there are challenges to solve to reduce costs and increase the competitiveness of this technology. One of them is the choice of condensation system. CSP/STE plants are currently designed with either cooling towers or air-cooled condensers. The efficiency of a CSP plant is defined, in large part, by the pressure and the temperature of the steam both entering and leaving the turbine. The steam conditions at the turbine outlet are defined by the temperature at which the steam is condensed. The lowest ambient temperature available is the wet bulb temperature; thus, most power plants use an evaporation process to provide the cooling water source for the condenser. The effect of the variation of the condensation temperature on the power produced by the plant can be 0.5%–1% per degree Celsius, [2]. Although cooling towers allow a lower level in the condensation temperature and, therefore, a higher thermal efficiency, there are drawbacks to be considered in the design phase of a plant. Firstly, water consumption, in the order of 2.3–3.4 m^3/h per MWe, [3]. It should be noted that the geographic areas where CSP plants are most productive, with high levels of direct irradiance, are often places with water shortages. Water consumption in cooling towers is used to compensate for the evaporation, the drain needed to maintain water quality and the drift. This last term, although not excessive, of the order of 0.001% of the recirculated water, is a problem by the emission of chemicals and microorganisms to the atmosphere like the bacterium Legionella. A potential approach toward eliminating or dramatically reducing water use in steam condensation is to use air-cooled steam condensers. Air cooled steam condensers (ACC), installed only in a low percentage of CSP plants, are a water-efficient option. Another advantage is to eliminate the plume, which is produced in the outlet section of the cooling tower in cold periods by mixing the stream of the humid outlet air and the ambient air. Particularly relevant in CSP plants, since the presence of the plume can reduce the efficiency of the collectors closer to the cooling tower. On the contrary, dry systems lead to a power production penalty on hot days, and higher capital costs compared to current cooling tower and water cooled surface condenser systems. Comparative studies of dry and wet condensation systems for the heat dissipation in CSP plants have been found in the literature [4]. presented a comparative overview of wet and dry cooling systems for Rankine cycle based CSP plants. They concluded that dry systems offer significant reductions in plant water usage compared to the circulating evaporative systems which are currently employed for CSP plant cooling. This could potentially lead to net plant capital cost and electricity unit cost reductions. However, the integration of direct ACC cooling systems results in overall plant efficiency reductions (which are bigger for parabolic trough CSP plants) ranging from 1% to 5% and to overall capital cost increase (ranging from 1% to 4%), due to increased cost of condenser material.

[5] compared the exergy destruction and exergetic efficiency of two different cooling technologies for a power cycle of 50 MWe in a thermal power plant. The simulations were carried out in two scenarios, considering that both technologies operate with the same parameters. Furthermore, the condensation pressure was fixed previously using also the same value in each cooling device. Due to this fact, the proper characteristics and limitations of each cooling device were not considered during the comparatives for a realistic performance of the power plant. They realised that the condenser is the component where more exergy of the total fuel exergy is wasted as exergy destruction. Additionally, they concluded that, from an exergetic point of view, the use of an air cooled condenser is not an efficient solution to work at low exit turbine pressures [6]. studied a direct steam generation in a trough-based CSP and conducted an energy and exergy analysis for different plant components. They also reported that maximum energy loss occurred in the condenser and the PTCs solar field [7]. undertook a detailed energy and heat transfer analysis for a 30 MWe CSP plant using EES and TRNSYS softwares. In an attempt to reduce the plant water requirement, the impact of replacing the wet cooling system with an air-cooled condenser was examined, and the results showed a considerable reduction in the power output which was estimated to be

1.3 MW. This is due to the increase in the condensation pressure and temperature. More recently [8], assessed relative techno-economics and net life cycle CO_2-eq emissions mitigation (LCCM) potential for 50 MWe nominal capacity wet-cooled and dry-cooled parabolic trough solar collector (PTSC) and dry-cooled solar power tower (SPT) based CSP plants with 6.0 h of thermal energy storage for two potential locations in India. It was observed that though dry cooling is likely to save significant amount of water (92%) in PTSC based plants, the same shall result in higher capital cost, higher performance penalty and higher parasitic power requirements leading to around 20% higher levelized cost of electricity (LCOE) as compared to wet-cooled PTSC based plants. While these studies show interesting conclusions, we consider that a more complete and current comparison should include hybrid systems, following the suggestion of [9]. Many efforts have been made over the past decades to improve the performance of dry cooling systems in order to make them more efficient compared to wet cooling. A number of studies have found that hybrid cooling technologies have the potential to alleviate this problem while avoiding issues related to wet cooling, particularly in terms of water utilisation. Some authors use the term hybrid systems for the simultaneous installation of wet and dry cooling towers in parallel and the choice of one system or another depending on the environmental conditions, [10]. This achieves savings in water consumption of more than 70% without excessively penalising the production of the plant, barely 3% [11]. investigated the water consumption in a hybrid cooling tower and concluded that the water consumption can be reduced by 75% and 65% in the case of parallel and series configurations, respectively, when the hybrid ratio is varied from 0.2 to 0.8. However, they observed that a higher heat transfer area is required in the dry cooler because of lower thermal efficiency [12]. analysed a hybrid cooling system to enhance the net power output of an air-cooled geothermal power plant. They considered evaporative pre-cooling of the ACC inlet air and the use of a water-cooled condenser in parallel or series with the ACC/Heller system to mitigate losses in power production by splitting the total condenser load. They reported that pre-cooling of the ACC inlet air can drop the air temperature close to its wet-bulb temperature with an effectiveness of about 75% [13]. studied the thermodynamic performance of a steam power plant with a combination of dry and wet cooling systems at different operating conditions and reported that the ACC is the best way to reject heat if the ambient temperature is lower than 16 C at 300 MWe, 24 C at 225 MWe and 31 C at 150 MWe [14]. performed numerical study to investigate pre-cooling of inlet air using Munters media and study its effect on the performance of a Natural Draft Dry Cooling Tower (NDDCT). They reported that the performance of NDDCT can be enhanced by pre-cooling inlet air with wetted media when the ambient air is hot and dry. However, at lower temperatures pre-cooling application does not benefit NDDCT performance. In another study [15], carried out a comparative study on the performance of natural draft dry, pre-cooled and wet cooling towers and showed that the pre-cooling enhancement can go up to 46% by increasing the NDDCT heat rejection rate from 93 MW to 136 MW in the hottest month [16]. studied hybrid cooling system technologies to study the performance improvement at high ambient temperatures and reported that hybrid system consumes less water than a wet cooling tower-only system, with estimated savings of 22–89% over ambient temperatures of 0–50 C [17]. developed the power block model of a 50 MWe CSP plant integrated with a hybrid cooling system to study the thermodynamic and water consumption performance of series, parallel, series-parallel, and parallel-series configurations at different operating conditions. They observed that the parallel configuration was promising in terms of power generation. However, the series-parallel configuration was the most favourable configuration in terms of water saving, resulting in 50% of water consumption reduction when compared to the only-wet cooling option [18]. reviewed several hybrid cooling approaches developed to boost the performance during hottest hours by introducing a small amount of water for a limited time to cool the entering air. According to Ref. [14]; there are two methods that carry out this concept which can be classified as deluge cooling and evaporative pre-cooling (spray cooling and wetted-media cooling). Regarding to deluge cooling, due to the direct contact of water with heat exchanger bundles, corrosion and fouling become crucial issues. This requires using treated water and regular cleaning or utilising condenser tubes with galvanic corrosion protection which prevents the use of fins. Wetted-media cooling also is an efficient way to cool inlet air. But, significant pressure drop is created which reduce air mass-flow rate causing a decline in heat rejection rate. Therefore, the optimal design of this type of hybrid system implies the search for a compromise between cooling efficiency and pressure loss. Over the past decades, pre-cooling methods have been used frequently in refrigeration cycles, [19]. However, this successful strategy has not carried over to CSP plants. Up until now, there have been limited studies undertaken on the energetic/exergetic performance and water consumption of the CSP plants including hybrid refrigeration systems.

This paper deals with the comparison of three condensation systems for the heat dissipation in a CSP/STE plant: wet system, dry system and hybrid system based on the pre-cooling of the air in an adiabatic panel located in the entrance section of a dry system. The study of the above mentioned hybrid system constituted the main novelty of this work. Energy, exergy and environmental (3E) analyses were conducted to assess the influence of the condensation system on the power plant performance. Secondary objectives include defining a selection criteria of the type and thickness of the evaporative pad for the hybrid system and assessing the influence of environmental conditions on the plant performance throughout the year.

2. Methodology

2.1. Plant description

The Andasol I is used as a real reference case of a concentrated solar power station. A conventional, reheated Rankine cycle coupled with a parabolic trough solar field is used to generate a net power capacity of 50 MWe.

The heat collected in the solar field by the heat transfer fluid, constitutes the energy source for the power cycle. The heat transfer fluid is pumped to the steam generator that consists of three heat exchangers arranged in series, economiser, steam generator and superheater, as well as a reheater in parallel with the other three heat exchangers.

The steam generator receives pre-heated feedwater and generates the steam required for the power cycle. The superheated steam

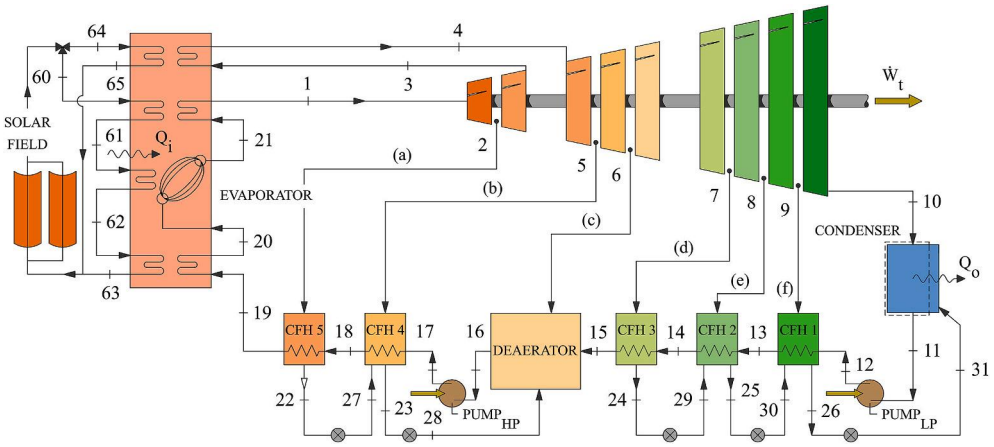

Fig. 1. Schematic arrangement of the Rankine cycle in Andasol I power plant.

expands in the high-pressure turbine. One extraction is taken and used to preheat feedwater in a closed feedwater heater. Upon exiting the high-pressure turbine, the steam is directed through a reheater, where it is superheated. The superheated steam at an intermediate pressure is expanded in the low-pressure turbine. Five extractions are taken from this stage of the turbine: one directed to an open feedwater heater (deaerator) and the remaining four to closed feedwater heaters, all of them used to preheat feedwater. The steam leaving the turbine is condensed and pumped twice in order to meet the pressure level requirements at the heaters and steam generator. A schematic arrangement of the power plant's cycle is depicted in Fig. 1, where all the components mentioned above can be found and the state points have been labelled.

2.2. Thermodynamic modelling

This section includes the major equations used in the analytical investigation conducted in this paper. Since the main objective of this work was to analyse the influence of the condensing system on the plant performance, attention was primarily paid to the Rankine cycle and condenser models. The solar field was considered in the analysis as a constant rate of heat input.

2.2.1. Plant modelling

The mass, energy and exergy balances (set of Eqs. (1)–(3)) were applied to all the components in the cycle to solve the transfer processes taken place in each one of them.

$$\frac{dm}{dt} = \sum_i \dot{m}_i - \sum_o \dot{m}_o \tag{1}$$

$$\frac{dE_{cv}}{dt} = \dot{Q} - \dot{W} + \sum_i \dot{m}_i \left(h_i + \frac{V_i^2}{2} + g z_i \right) - \sum_o \dot{m}_o \left(h_o + \frac{V_o^2}{2} + g z_o \right) \tag{2}$$

$$\frac{d\mathrm{Ex}_{cv}}{dt} = \sum_j \left(1 - \frac{T_0}{T_j} \right) \dot{Q}_j - \left(\dot{W} - p_0 \frac{dV_{cv}}{dt} \right) + \sum_i \dot{m}_i \mathrm{ex}_i - \sum_o \dot{m}_o \mathrm{ex}_o - \dot{\mathrm{E}}\mathrm{x}_d \tag{3}$$

where the subscript 0 refers to the dead state and ex is the specific flow exergy. This exergy is constituted by the sum of two contributions: the *thermomechanical* and the *chemical* exergies. They physically represent the maximum amount of work realisable when the substances in a control mass are allowed to pass into the environment and through chemical reaction, respectively. According to Ref. [20]; the specific flow exergy (or availability) for a stream of water vapour or liquid water can be expressed as:

$$\mathrm{ex} = \left[h(T,p) - h_g(T_0) \right] - T_0 \left[s(T,p) - s_g(T_0) \right] + \frac{v^2}{2} + g z - R_v T_0 \ln \left(\frac{x_v^0 p_0}{p_g(T_0)} \right) \tag{4}$$

Eq. (4) can be simplified in the case of an incompressible liquid only stream,

$$\mathrm{ex} = \left[h_f(T) - h_g(T_0) \right] + v_f \left[p - p_g(T) \right] - T_0 \left[s_f(T) - s_g(T_0) \right] - R_v T_0 \ln \left(\frac{x_v^0 p_0}{p_g(T_0)} \right) \tag{5}$$

where kinetic and potential energy terms are neglected. Finally, the flow exergy in the moist air stream interacting with the cycle in the cooling systems considered in the paper, was modelled as an ideal gas mixture involving a binary mixture of water vapour and dry air,

$$\mathrm{ex} = \left(c_{p_a} + \omega\, c_{p_v}\right) T_0 \left(\frac{T}{T_0} - 1 - \ln\frac{T}{T_0}\right) + (1+\widetilde{\omega})\, R_a\, T_0 \ln\frac{p}{p_0} + \\ + R_a\, T_0 \left[(1+\widetilde{\omega}) \ln\frac{1+\widetilde{\omega}_0}{1+\widetilde{\omega}} + \widetilde{\omega} \ln\frac{\widetilde{\omega}}{\widetilde{\omega}_0}\right] \tag{6}$$

The following major assumptions were considered in order to simplify the balances:

- Steady state operation.
- Negligible changes in potential and kinetic energy of fluid streams.
- All the components are adiabatic except the steam generator system and the condenser.
- Feedwater leaves the preheater as saturated liquid ($x = 0$).
- Steam leaves the steam generator as saturated vapour ($x = 1$).
- Feedwater exits the condenser as saturated liquid ($x = 0$).
- Condensed steam exits the open feedwater heater (deaearator) as saturated liquid ($x = 0$).

As a result, the simplified mass and energy equations for the processes taken place in all the elements in the cycle, are shown in Table 1. The bleds in each one of the stages of the low pressure turbine are referred as a to f (see Fig. 1).

The performance of each stage of the turbines and the pumps is modelled by the isentropic efficiency. Both open and closed feedwater heaters are modelled via the Terminal Temperature Difference (TTD) and the Drain Cooler Approach (DCA). The former is defined as the inlet steam saturation temperature and feedwater outlet temperature difference, while the latter can be expressed as the exchanger drain outlet temperature and feedwater inlet temperature difference.

Concerning the exergy analysis, the percent exergy destruction rate in each system component, y_D, compares the exergy destruction rate in a component ($\dot{\mathrm{E}}\mathrm{x}_{\mathrm{d},\ \mathrm{k}}$) with the rate of exergy supplied to the system [21],

$$y_D = 100\frac{\dot{\mathrm{E}}\mathrm{x}_{\mathrm{d},\ \mathrm{k}}}{\dot{\mathrm{E}}\mathrm{x}_{\mathrm{i}}} \tag{7}$$

Alternatively, the component exergy destruction rate can be compared with the total exergy destruction rate within the system, $\dot{\mathrm{E}}\mathrm{x}_d$, giving the ratio:

$$y_{D_k} = 100\frac{\dot{\mathrm{E}}\mathrm{x}_{\mathrm{d},\ \mathrm{k}}}{\dot{\mathrm{E}}\mathrm{x}_{\mathrm{d}}} \tag{8}$$

Finally, the energetic and exergetic efficiencies of the cycle and the plant are defined. Regarding the cycle, these definitions can be expressed as shown in Eqs. 9 and 10:

$$\eta_{\mathrm{cycle}} = 100\frac{\dot{W}_{\mathrm{gross}}}{\dot{Q}_{\mathrm{i}}} \tag{9}$$

Table 1
Energy balance in the components present in the cycle.

Component	Energy balance
HP Turbine	$\frac{\dot{W}_{\mathrm{tHP}}}{\dot{m}_1} = (h_1 - h_2) + (1-\mathrm{a})(h_2 - h_3)$
IP Turbine	$\frac{\dot{W}_{\mathrm{tIP}}}{\dot{m}_1} = (1-\mathrm{a})(h_4 - h_5) + (1-\mathrm{a}-\mathrm{b})(h_5 - h_6)$
LP Turbine	$\frac{\dot{W}_{\mathrm{tLP}}}{\dot{m}_1} = (1-\mathrm{a}-\mathrm{b}-\mathrm{c})(h_6 - h_7) + (1-\mathrm{a}-\mathrm{b}-\mathrm{c}-\mathrm{d})(h_7 - h_8) + + (1-\mathrm{a}-\mathrm{b}-\mathrm{c}-\mathrm{d}-\mathrm{e})(h_8 - h_9) + (1-\mathrm{a}-\mathrm{b}-\mathrm{c}-\mathrm{d}-\mathrm{e}-\mathrm{f})(h_9 - h_{10})$
Condenser	$\frac{\dot{Q}}{\dot{m}_1} = (1-\mathrm{a}-\mathrm{b}-\mathrm{c}-\mathrm{d}-\mathrm{e}-\mathrm{f})h_{10} + (\mathrm{d}+\mathrm{e}+\mathrm{f})h_{31} - (1-\mathrm{a}-\mathrm{b}-\mathrm{c})h_{11}$
HP Pump	$\frac{\dot{W}_{\mathrm{pHP}}}{\dot{m}_1} = (h_{17} - h_{16})$
LP Pump	$\frac{\dot{W}_{\mathrm{pLP}}}{\dot{m}_1} = (1-\mathrm{a}-\mathrm{b}-\mathrm{c})(h_{12} - h_{11})$
CFH 1	$(1-\mathrm{a}-\mathrm{b}-\mathrm{c})(h_{12} - h_{13}) + (\mathrm{d}+\mathrm{e})h_{30} + fh_9 - (\mathrm{d}+\mathrm{e}+\mathrm{f})h_{26} = 0$
CFH 2	$(1-\mathrm{a}-\mathrm{b}-\mathrm{c})(h_{13} - h_{14}) + dh_{29} + eh_8 - (\mathrm{d}+\mathrm{e})h_{25} = 0$
CFH 3	$(1-\mathrm{a}-\mathrm{b}-\mathrm{c})(h_{14} - h_{15}) + \mathrm{d}(h_7 - h_{24}) = 0$
CFH 4	$(h_{17} - h_{18}) + ah_{27} + bh_5 - (\mathrm{a}+\mathrm{b})h_{23} = 0$
CFH 5	$(h_{18} - h_{19}) + \mathrm{a}(h_2 - h_{22}) = 0$
Deaerator	$(\mathrm{a}+\mathrm{b})h_{28} + ch_6 + (1-\mathrm{a}-\mathrm{b}-\mathrm{c})h_{15} - h_{16} = 0$

$$\varepsilon_{\text{cycle}} = 100\frac{\dot{W}_{\text{gross}}}{\dot{\text{Ex}}_{\text{i}}} \tag{10}$$

Here, $\dot{W}_{\text{gross}}$ is the difference between the power generated by the turbines and the power absorbed by the pumps. The overall plant efficiencies are expressible as:

$$\eta_{\text{plant}} = 100\frac{\dot{W}_{\text{net}}}{\dot{Q}_{\text{i}}} \tag{11}$$

$$\varepsilon_{\text{plant}} = 100\frac{\dot{W}_{\text{net}}}{\dot{\text{Ex}}_{\text{i}}} = 100\left(1 - \frac{\dot{\text{Ex}}_{d}}{\dot{\text{Ex}}_{\text{i}}}\right) \tag{12}$$

where the net power production includes the consumption of the auxiliary elements of the cooling system.

2.2.2. Modelling of the cooling systems

Three different cooling systems were considered in the comparative study: wet (cooling tower), dry (air-cooled condenser) and hybrid (air-cooled condenser with a wetted-media evaporative pre-cooling). The performance of these devices is modelled via the Initial Temperature Difference (ITD). It is the difference between the condensing temperature and the minimum temperature reachable for each technology, [2].

2.2.2.1. Cooling tower. In a wet cooling tower, the heat collected from the condenser is rejected to the atmosphere mainly by means of evaporation. Fig. 2 shows a schematic arrangement of the condenser and cooling tower interaction. Cooling tower performance relies on the ambient air wet bulb temperature. Accordingly, ITD is calculated as the difference between the condensing temperature and the ambient air wet-bulb temperature:

$$ITD = T_{\text{cond}} - T_{wb} = \left(T_{w,i} - T_{w,o}\right) + \left(T_{\text{cond}} - T_{w,i}\right) + \left(T_{w,o} - T_{wb}\right) \tag{13}$$

where $(T_{w,i} - T_{w,o})$ is the range and $(T_{\text{cond}} - T_{w,i})$ is the TTD. Typical operation values of ITD = 16 C, Range = 8 C and TTD = 2 C were considered in the simulations. The condensing pressure and therefore the power plant efficiency can be calculated once the condensing temperature is known.

Regarding the power consumption of the auxiliary equipment, a cooling tower composed by five cells and a circulation pump was considered. The pump power consumption was obtained using the circulated volumetric flowrate (calculated via the rejection heat rate and the cooling tower range) and the pump pressure difference [5]. The power consumed by the fans was obtained from the same reference. Each of the tower cells works with a 100-kW fan, for a total of $\dot{W}_{\text{fan, wet}} = 500$ kW.

The other variable used to compare the plant performance using different cooling systems is the water consumption. One of the main issues of evaporative devices is the large amount of water lost by evaporation. With regard to cooling tower water consumption, 3 losses have been considered: evaporation, drift and blowdown. Other losses such as process leaks or cleaning have been neglected. Evaporated water has been calculated by using the [22] theory for the thermal evaluation of cooling towers. The authors derived the governing equations of heat and mass transfer for a counterflow cooling tower configuration, set of equations 14–16:

$$\frac{dw}{dT_w} = c_{p_w}\frac{\dot{m}_w}{\dot{m}_a}(w_{s_w} - w)\times \frac{1}{h_{s_w} - h + (Le-1)[h_{s_w} - h - (w_{s_w} - w)h_v] - (w_{s_w} - w)c_{p_w}T_w} \tag{14}$$

$$\frac{dh}{dT_w} = \frac{\dot{m}_w c_{p_w}}{\dot{m}_a}\times \left(1 + \frac{(w_{s_w} - w)c_{p_w}T_w}{h_{s_w} - h + (Le-1)[h_{s_w} - h - (w_{s_w} - w)h_v] - (w_{s_w} - w)c_{p_w}T_w}\right) \tag{15}$$

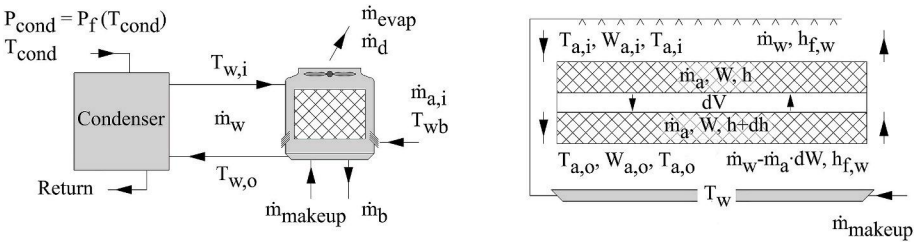

Fig. 2. Schematic arrangement of the cooling tower and energy and mass balances for evaporated water.

$$\frac{dMe_P}{dT_w} = c_{p_w} \times \frac{1}{h_{s_w} - h + (Le-1)[h_{s_w} - h - (w_{s_w} - w)h_v] - (w_{s_w} - w)c_{p_w}T_w} \tag{16}$$

Therefore, by solving this set of equations, the evolution of the air properties, such as the humidity, through the entire cooling process can be predicted by the Poppe approach. As a result, the evaporated water can be calculated as shown in Eq (17).

$$\dot{m}_{\text{evap}} = \dot{m}_a\left(\omega_{a,\text{evap}} - \omega_{\text{amb}}\right) \tag{17}$$

According to the literature, Poppe formulation resulted in values of evaporated water flow rate that were in good agreement with full scale cooling tower test results, [23].

Drift losses refer to the amount of total tower water flow escaping the cooling tower and are usually expressed as the ratio between the mass flow of water escaping from the tower ($\dot{m}_d$) and the total mass flow recirculated by the tower ($\dot{m}_w$),

$$D = 100\frac{\dot{m}_d}{\dot{m}_w} \tag{18}$$

In this work a drift rate of $D = 0.0005\%$ was considered as for a typical present-day manufacturers' guaranteed drift rates, [24].

Finally, blowdown losses ($\dot{m}_b$) refer to the dissolved solids remaining in the recirculating water when water evaporates from the tower. The blowdown losses can be calculated taking into account the cooling tower cycles of concentration (C_c). Cycles of concentration represent the accumulation of dissolved minerals in the recirculating cooling water ($C_c = 6$ was assumed in this work as a typical design value in Spain). Analytically, $\dot{m}_b$ can be estimated as,

$$\dot{m}_b = \frac{\dot{m}_{\text{evap}} + \dot{m}_d}{C_c - 1} \tag{19}$$

2.2.2.2. Dry system. In air-cooled systems, the waste heat from the condenser is transferred by convection. Hence, this kind of systems depend on the ambient air dry-bulb temperature rather than the ambient air wet-bulb temperature. Fig. 3 shows a schematic arrangement of the condenser and dry system interaction. As in the case of the wet system, the dry system was modelled through the ITD approach, though in this case, the condensing temperature was limited to the ambient dry air temperature,

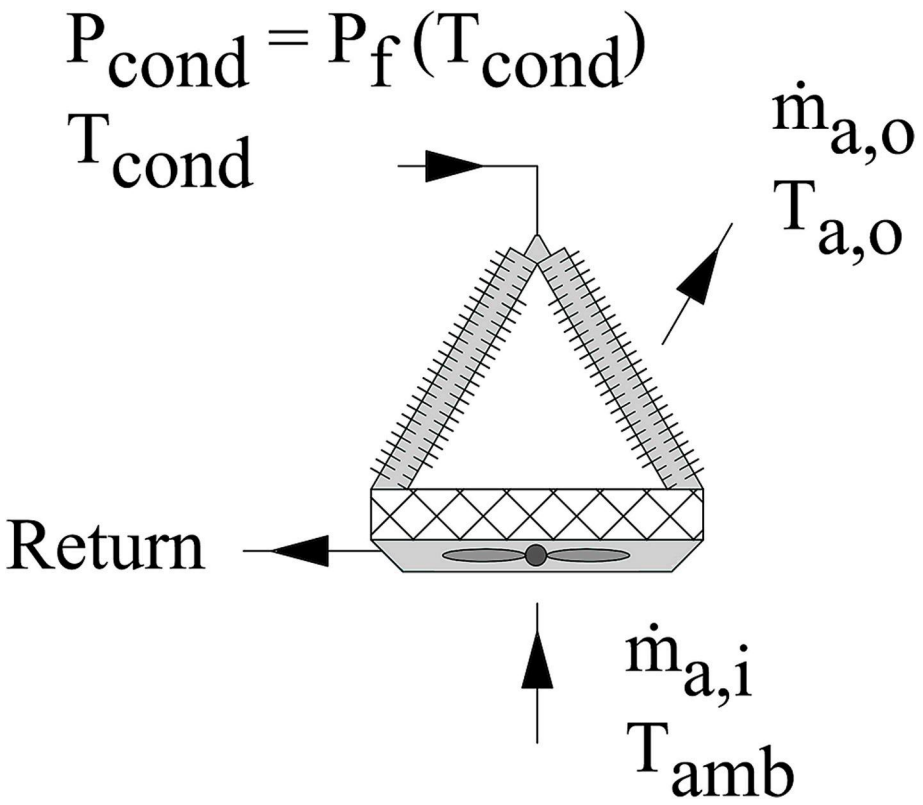

Fig. 3. Schematic arrangement of the dry system.

$$ITD = T_{\text{cond}} - T_{\text{amb}} \tag{20}$$

Another parameter taken into account was the air difference temperature, defined as the difference between inlet and outlet temperatures, $\Delta T_{\text{air}} = T_{a,o} - T_{a,i}$. An ITD = 22 C and $\Delta T_{\text{air}} = 15.15$ C were considered according to Ref. [2]. As in the cooling tower model, the power consumption in the air condenser was taken from the work of [5]. In this case, the fan consumption is $\dot{W}_{\text{fan, dry}} =$ 4066.8 kW.

2.2.2.3. Hybrid system. By including the media pad in an air-cooled condenser, the condensing pressure of the cycle decreases, thus increasing the efficiency of the cycle. Finally, the rejected heat leaves the device as warm air. Fig. 4 shows the hybrid system based on the wetted-media pad evaporative pre-cooling method linked to the power cycle condenser. Moreover, the evolution of the psychrometric variables is depicted in the psychrometric chart.

The cooling efficiency of an evaporative pad is defined as the ratio between the actual temperature difference at the evaporative section to the lowest attainable temperature difference (wet-bulb temperature).

$$\epsilon = \frac{T_{\text{amb}} - T_{a,i}}{T_{\text{amb}} - T_{wb}} \tag{21}$$

According to several authors [25–27], the evaporative cooling efficiency can be modelled as a function of the convective heat transfer coefficient, the airflow properties and the geometric characteristics of the evaporative pad as follows:

$$\epsilon = 1 - e^{\left(-\frac{\beta\delta}{V^{\alpha}}\right)} \tag{22}$$

where δ represents the thickness of the pad, V is the measured frontal velocity of the air stream and α and β are constants. The pressure drop can be expressed as a function of the air velocity, as in Eq. (23):

$$\Delta p = kV^2 \tag{23}$$

The power consumption of the hybrid system fan was defined taking the dry system as a reference and including the additional pressure induced by the cooling pad:

$$\dot{W}_{\text{fan, hybrid}} = \dot{W}_{\text{fan, dry}}\left(1 + \frac{\Delta p}{\Delta p_{\text{air}}}\right) \tag{24}$$

where Δp_{air} is the pressure drop in the dry system and Δp is the extra pressure drop induced by the pad.

In order to select the best cooling pad for this application, an optimisation analysis was carried out. The description of the procedure and the results are shown in A, where several cooling pads manufactured by Munters (CELdek evaporative cooling pads) were analysed. The pad chosen to carry out the comparative was the model 7090-15 with a thickness of 0.2 m. The constants in Eqs. (22) and (23) are $\alpha = 0.26$, $\beta = 13.2$ and $k = 17.84$. The air velocity was set to 1 m/s.

Once the evaporative section exit temperature ($T_{a,i}$) is known, the calculation procedure is the same than the one for the dry system replacing the intermediate temperature by the ambient temperature (ITD = 18 C and $\Delta T_{\text{air}} = 15.15$ C). Concerning the water consumption, in this case just the water lost due to the evaporation is considered. It can be estimated as in the wet system by Eq. (17).

2.2.3. Model validation

The set of equations displayed in Table 1 was solved by means of Engineering Equation Solver (EES) software, (F-Chart Software, 2016). This software allows the calculation of the thermodynamic properties of different fluids.

The model was defined using technical data of the thermal solar plant of Andasol-I at nominal conditions, [5]. Table 2 provides an overview of the main parameters and the major assumptions used in the thermodynamic simulations. Further information is given in this subsection.

Inlet temperatures to the first and second stages of the turbine were set to 373 and 373.4 C, respectively, whereas the outlet temperatures for economiser and the steam generator were 309 and 313 C. With regard to the pressure levels, the output pressure of the first turbine stage and the condensation pressure were 18.5 and 0.0603 bar. The pressure level of each of the six extractions was

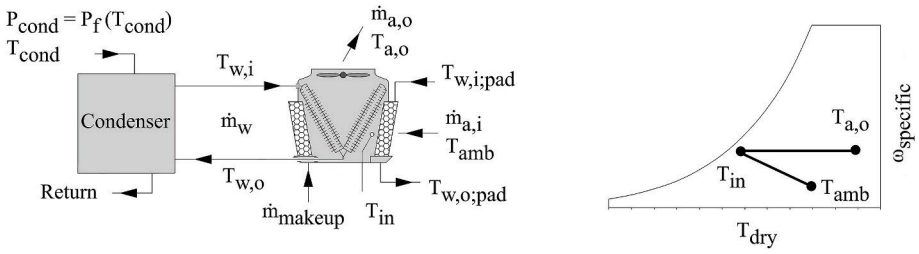

Fig. 4. Schematic arrangement of the hybrid system and psychrometric chart.

Table 2
Main parameters used in the simulations.

Isentropic efficiencies (–)	
High pressure turbine isentropic efficiency	0.852
Intermediate pressure turbine isentropic efficiency	0.90
Low pressure turbine isentropic efficiency	0.852
Low pressure/cooling tower Pump isentropic efficiencies	0.73
High pressure Pump isentropic efficiencies	0.81
Extraction pressure level, by destination (bar)	
Feedwater heater number 1 (closed)	0.37
Feedwater heater number 2 (closed)	1.17
Feedwater heater number 3 (closed)	3.04
Feedwater heater number 4 (closed)	13.99
Feedwater heater number 5 (closed)	33.48
Deaerator	6.18
Feedwater heaters (heat exchangers) (C)	
Drain Cooler Approach	5
Terminal Temperature Difference	4
Thermodynamic properties at main locations	
Steam generation pressure level, p_1 (bar)	4

33.48, 13.99, 6.18, 3.04, 1.17 and 0.37 bar respectively, and the discharge pressures of the high and low pumps were set to 103 and 8.38 bar. In this work, it was considered that the extraction pressures remain constant regardless of the simulated condensation system (condensation pressure). An example of how to solve the mass and energy balances for the feedwater heaters in a hybrid geothermal–fossil power generation system can be found in Ref. [28]. Moreover, the isentropic efficiencies of the pumps were 0.81 and 0.73 (high and low pressure). Heat exchangers were modelled via the Terminal Temperature Difference (TTD = 4 C) and the Drain Cooler Approach (DCA = 5 C).

A wet cooling system (cooling tower) was considered in the simulations at the validation stage. The cooling tower range and approach were set to 9.7 and 6.8 C respectively, and the ambient conditions were 20 C (dry temperature) and 50% of relative humidity.

Fig. 5 shows the comparison between the $T - s$ diagrams for the Rankine cycle reported by Ref. [5] and the one obtained in this research. As it can be seen, an excellent agreement is observed between them. Differences lower than 1% regarding the main parameters of the cycle (thermal efficiency, mass flow rates, heat rates, etc.) were found. Therefore, in the light of the results shown, the model was considered validated.

3. Results and discussion

The objective of this section is to show and discuss the differences in energy conversion, exergy destruction and water use for the

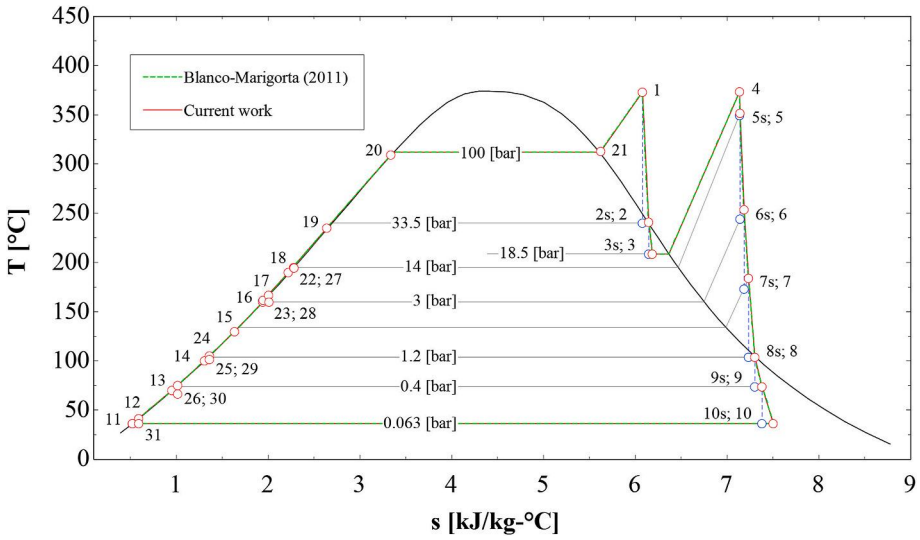

Fig. 5. $T - s$ diagram of the cycle for the validation stage.

studied condensation systems. As previously stated, the solar field was modelled as a constant input rate of heat and a temperature difference based on the ITD was defined for the condenser-cooling system interaction.

Tables 3 and 4 show the results obtained in the simulations for each condensation system analysed (wet, hybrid and dry).

3.1. Energy analysis

For the comparison, the dry heat dissipation system consisting of an air-cooled condenser has been taken as the base case.

The power produced in the high pressure turbine is the same in all three cases. This is because all the extractions made to feed the closed exchangers are carried out at the same pressure and temperature. In the low-pressure stages occurs in a similar way, with the exception that the steam expands in the last stage to the pressure of condensation established by the operating conditions of each of the three technologies. Fig. 6 shows the $T - s$ diagram of the three configurations. It should be noted that point 10, which represents the condensation conditions, is the variable influenced by each refrigeration system considered. As can be seen, as the pressure decreases, the area of the cycle increases and therefore the power generated will increase. This variation in the condensation pressures leads to a increase in the total power generated by the turbines, of the order of 5.66% in the wet system and 4.62% in the hybrid system with respect to the dry system.

With regard to the consumption of the auxiliary elements of the plant, this is comprised by the consumption of the recirculation pumps and the fans of the refrigeration systems. The wet system has the recirculation pumps and the cooling tower fans, while the other two systems use only fans to carry out the same task because they are aero-condensers. The difference between the air and water specific heats involves a higher air mass flow rate to dump the heat to the atmosphere. This fact implies a higher energy consumption in the fans of the hybrid and dry refrigeration systems. This variation has been quantified in a consumption 3.01 times greater for the hybrid system and 2.89 times greater for the dry system with respect to the wet one. The fact that the consumption in the hybrid system is higher than the dry one is caused by the pressure loss generated by the presence of the evaporative panels to reduce the inlet temperature of the cooling air.

With respect to the gross and net power (power generated in the turbines minus the consumption of the auxiliary elements), the percentage variation between them for each heat dissipation system is 1.48% for the wet system, 7.51% for the hybrid system and 7.48% for the dry system. Comparing the net power produced by the three systems, an increment in power generation is obtained with a percentage variation of 12.60% and 4.65% for the wet and hybrid system respectively with respect to the dry one. The fact that the hybrid system has a greater production of net power with respect to the dry system is due to the low condensation pressures that are achieved with the hybrid configuration. Even though the hybrid system has a higher consumption in the auxiliary elements it is still more competitive. In line with the rest of the results obtained at the energy level, the energy performance of the plant with cooling tower shows better results, followed by the hybrid system and the dry one.

3.2. Exergy analysis

In this subsection, a study of the power plant is carried out taking into account the exergy destruction, the exergy destruction ratio, the exergy destruction rate, and the exergy efficiency in each component, as shown in Table 4. As the input heat provided by the solar field is the same for the three cases of study, there is no special differences in exergy between the majority of the components in the

Table 3
Energy comparative results.

Component	Wet	Hybrid	Dry
High pressure turbine (kW)	17473.63	17473.63	17473.63
Low pressure turbine (kW)	40883.20	40309.42	37758.21
Condenser pump (kW)	−55.72	−55.71	−55.61
Feedwater pump (kW)	−791.37	−791.37	−791.37
Coolint tower pump (kW)	−352.98	–	–
Fan (kW)	−500.00	−4277.25	−4066.80
Reheater (kW)	26284.65	26284.65	26284.65
Superheater (kW)	16625.35	16625.35	16625.35
Evaporator (kW)	80322.07	80322.04	80322.07
Economiser (kW)	22871.59	22871.59	22871.59
Solar field heat (kW)	146103.66	146103.63	146103.66
Heat rejected (kW)	88593.92	89167.66	91718.80
Condenser pressure (bar)	0.060	0.069	0.124
Gross power (kW)	57509.74	56935.94	54384.86
Net power (kW)	56656.76	52658.70	50318.06
Cycle efficiency (−)	0.394	0.390	0.372
Plant efficiency (−)	0.388	0.360	0.344
Evaporation water loss (kg/s)	35.72	12.12	–
Purge water loss (kg/s)	7.14	–	–
Drift water loss (kg/s)	0.01	–	–
Total water loss (kg/s)	42.88	12.12	–
Water usage ($m^3/h/MW_{net}$)	2.72	0.83	–

Table 4
Exergy comparative results.

	$\dot{E}x_d$ (kW)			y_D (%)			y_{D_k} (%)			ε(%)		
Component	Wet	Hybrid	Dry	Wet	Hybrid	Dry	Wet	Hybrid	Dry	Wet	Hybrid	Dry
High pressure turbine	1816.75	1816.74	1816.75	2.35	2.47	2.39	8.81	7.86	7.84	90.58	90.58	90.58
Low pressure turbine	4956.02	4847.67	4387.15	6.41	6.60	5.77	24.04	20.97	18.93	891.9	89.26	89.59
Condenser pump	14.65	14.53	14.00	0.02	0.02	0.02	0.07	0.06	0.06	73.71	73.92	74.83
Feedwater pump	105.33	105.33	105.33	0.14	0.14	0.14	0.51	0.45	0.46	86.69	86.69	86.69
Cooling tower pump	105.52	–	–	0.14	–	–	0.51	–	–	70.11	–	–
Reheater	2201.60	2201.58	2201.60	2.85	3.00	2.89	10.68	9.52	9.50	83.11	83.11	83.11
Superheater	756.77	756.87	756.77	0.98	1.03	0.99	3.67	3.27	3.26	91.72	91.72	91.72
Evaporator	3184.27	3184.72	3184.27	4.12	4.33	4.19	15.44	13.78	13.74	92.44	92.44	92.44
Economiser	1213.63	1213.79	1213.63	1.57	1.65	1.60	5.89	5.25	5.24	89.41	89.41	89.41
Condenser	1709.26	7660.84	8033.85	2.21	10.42	10.56	8.29	33.14	34.66	27.09	10.10	22.08
Cooling system	2883.64	7660.84	8033.85	3.73	10.42	10.56	13.99	33.14	34.66	40.43	10.10	22.08
IC1 (low pressure)	337.32	292.54	133.06	0.44	0.40	0.17	1.64	1.27	0.57	60.66	63.28	74.36
IC2 (low pressure)	243.40	243.40	243.40	0.31	0.33	0.32	1.18	1.05	1.05	79.98	79.98	79.98
IC3 (low pressure)	227.57	227.57	227.57	0.29	0.31	0.30	1.10	0.98	0.98	85.81	85.81	85.81
IC4 (high pressure)	267.82	267.82	267.82	0.35	0.36	0.35	1.30	1.16	1.16	90.08	90.08	90.08
IC5 (high pressure)	375.95	375.95	375.95	0.49	0.51	0.49	1.82	1.63	1.62	92.50	92.50	92.50
Deaerator	199.80	199.80	199.80	0.26	0.27	0.26	0.97	0.86	0.86	89.70	89.70	89.70
Total plant	20619.07	23119.18	23180.38	–	–	–	99.90	101.25	99.92	73.77	69.21	68.46

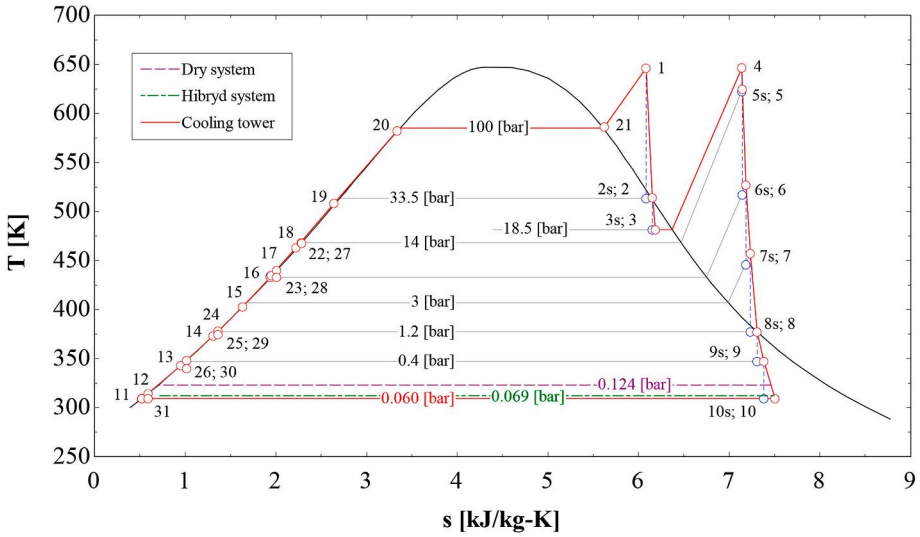

Fig. 6. $T - s$ diagram of the comparative for each cooling technology.

cycle, with exception of the low pressure turbine and the condenser.

The exergetic efficiency of each component assesses the fuel exergy wasted in the component as exergy destruction. Related to this parameter, Table 4 shows the following results:

The economiser shows an efficiency of 89%, the evaporator and superheater an efficiency of 92% and the reheater an efficiency of 83%. The sum of the overall exergy destructed for all these components and for the wet, hybrid and dry cooling system are: 35.68%, 31.82% and 31.73% respectively. The irreversibilities produced by these technologies can be explained by pressure and heat loss with the surroundings of the heat exchangers.

The amount of exergy destroyed in the turbine stages is very similar among the three studied condensation systems, with exergy performance of 91% for the high pressure stages and 89% for the low pressure stages. This is 32.85% for the wet system, 28.83% for the hybrid and 26.76% for the dry system with respect to the total exergy destroyed in the cycle.

In relation to the pumps used in the cycle, the exergy destroyed is the same, being the exergy efficiency of 74% for the condenser pump and 87% for the recirculation one. There is an exception in the wet system, where the circulation pump of the cooling tower is included in the cooling system. The exergy destroyed in these technologies is basically caused by friction.

The closed heat exchangers show a high exergy efficiency: between 60 and 70% for those installed in the output of the condenser and 80–90% for the other four ones. The exergy performance of the deaerator is 90%. All of these components represent with respect to the overall exergy destruction a 8.01% for the wet system, 6.95% for the hybrid one and 6.24% for the dry system. As it was explained

Table 5
Comparative results for each cooling technology per month.

Ambient conditions			Gross power (MW)			Net power (MW)			Plant efficiency			Water use (kg/s)		Exergetic efficiency		
Month	T_{amb} (K)	φ_{amb}	CT	D	H	CT	D	H	CT	D	H	CT	H	CT	D	H
January	279.7	0.72	61.03	59.22	60.56	60.19	55.16	56.30	0.412	0.378	0.385	27.10	4.72	0.761	0.701	0.709
February	281.6	0.67	60.74	58.80	60.26	59.91	54.73	56.00	0.410	0.375	0.383	28.54	5.93	0.759	0.700	0.707
March	284.6	0.59	60.33	58.13	59.83	59.49	54.07	55.57	0.407	0.370	0.380	30.93	8.40	0.756	0.698	0.704
April	286.5	0.57	60.02	57.71	59.51	59.18	53.64	55.25	0.405	0.367	0.378	32.28	9.39	0.753	0.696	0.705
May	290.4	0.51	59.46	56.83	58.92	58.61	52.77	54.66	0.401	0.361	0.374	35.32	12.39	0.749	0.693	0.698
June	295.5	0.44	58.77	55.68	58.20	57.92	51.62	53.93	0.396	0.353	0.369	39.49	16.66	0.743	0.689	0.691
July	298.5	0.38	58.48	55.00	57.88	57.63	50.93	53.61	0.394	0.349	0.367	42.36	20.31	0.739	0.687	0.685
August	298.0	0.42	58.40	55.12	57.82	57.56	51.05	53.55	0.394	0.349	0.367	41.47	18.44	0.740	0.687	0.688
September	294.3	0.52	58.71	55.95	58.16	57.86	51.89	53.89	0.396	0.355	0.369	37.76	13.52	0.745	0.690	0.695
October	289.2	0.64	59.33	57.10	58.82	58.48	53.04	54.55	0.400	0.363	0.373	33.36	8.52	0.751	0.694	0.701
November	283.8	0.72	60.21	58.31	59.73	59.36	54.24	55.46	0.406	0.371	0.380	29.51	5.48	0.756	0.698	0.706
December	280.8	0.76	60.73	58.98	60.26	59.89	54.91	56.00	0.410	0.376	0.383	27.51	4.16	0.760	0.700	0.708

previously, for the heat exchangers of the solar field, these losses can be justified due to pressure and heat loss between fluids.

The exergy destruction rate in the condenser using a cooling tower represents 22.28% of the total exergy destruction (including condenser, cooling tower and pump), using an hybrid condenser 33.14% whereas with an air cooled condenser it represents 34.66% of the total exergy destruction. In the case of the wet system, it represents the second process, after the low pressure turbine, where more exergy is destroyed. The hybrid and dry cooling systems are the devices that destroy more exergy in the power plant. This fact indicates that the condensation system using the cooling tower is the most efficient solution. Hybrid and dry systems present many irreversibilities due to the large amount of energy required to produce the mass flow of air needed for the heat exchange. These values represent almost a third of the total exergy destroyed in the global system. The exergetic performance of the cycle is 73.77% for the wet system, 69.21% for the hybrid and 68.46% for the dry system. This is due, as expected, the irreversibilities caused by each of the condensation systems.

3.3. Water use

To quantify the use of water for refrigeration, only the wet and hybrid system are taken into account since the dry system does not require direct water consumption in the condensation process. The cooling tower consumes 71.74% more water than the aero-cooler system with adiabatic pre-cooling. This is mainly because the cooling towers use the latent heat (evaporation) as the main means of heat dissipation, which causes a large amount of evaporated water. To evaluate the water consumption in the cooling towers, the water used in maintenance and purging tasks must be added in order to maintain the quality of the water in circulation. In addition, due to its operating principle there is an inevitable amount of water drift that is carried by the air stream. This water drift is not relevant quantitatively speaking, but it is when evaluating the environmental implications of wet systems. The distribution of water used in the cooling tower is 83.31% due to evaporation, 16.66% to purges and 0.03% to drift. The results show that the hybrid system reduces to almost one third the water consumption due to evaporation. In terms of water consumption per power generated, the wet system

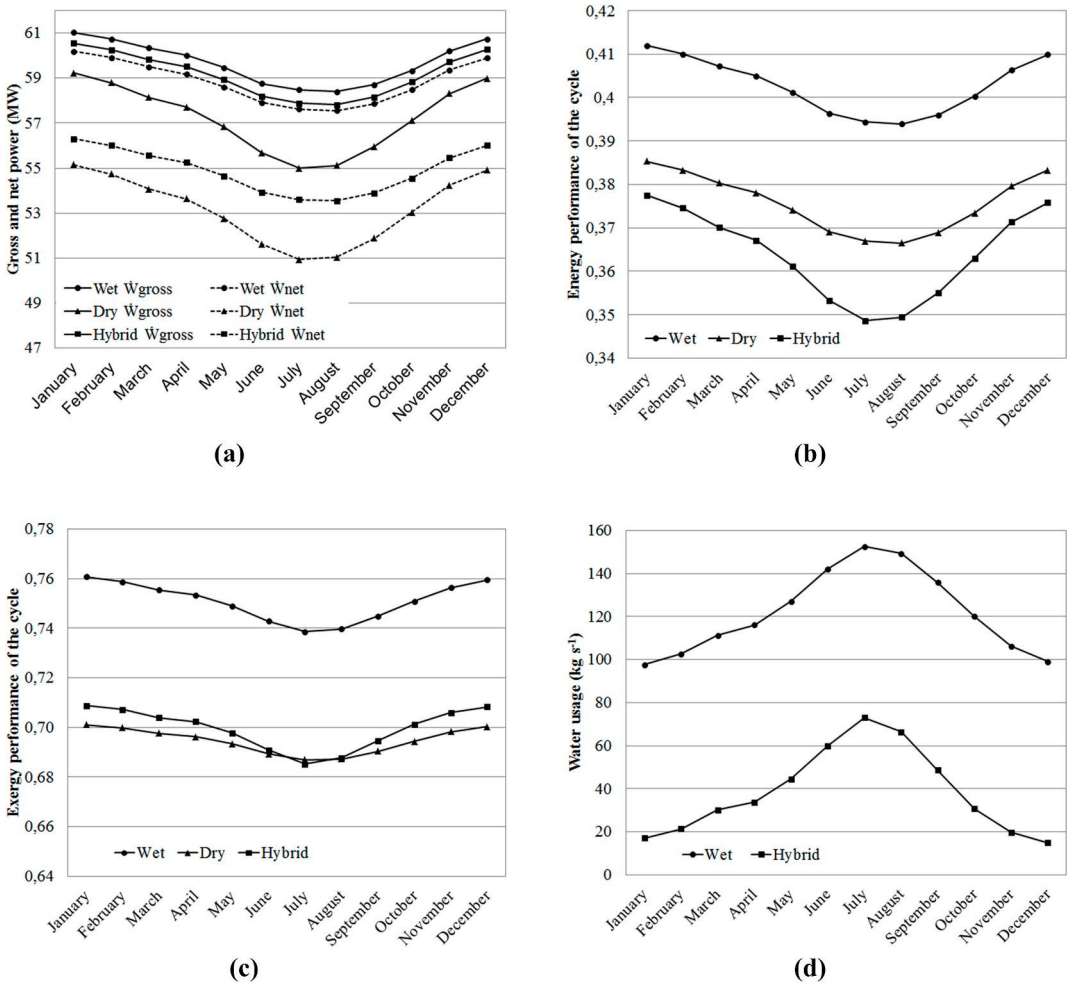

Fig. 7. a) $\dot{W}_{gross}$ and $\dot{W}_{net}$, b) energy efficiency, c) exergy efficiency and d) water usage.

requires 2.72 m^3 per MWh while the hybrid 0.83 m^3 per MWh, consistent with the data of other references, [2]. In relation to the emissions of the condensation systems, and particularly as regards to the problems of proliferation and dispersion of the Legionella, as previously anticipated, the cooling towers are classified as high-risk systems. On the contrary, the evaporative coolers included in the hybrid systems do not provide suitable growth conditions and generally do not release aerosol. A good maintenance program eliminates potential problems and reduces the concern of spread disease, [29].

3.4. Ambient conditions influence

In this section the ambient conditions influence on the thermal solar power plant is studied. To carry out the simulations, a constant and equal heat input by the solar field was considered. The results can be seen in Table 5. Weather data was taken from the Spanish State Meteorological Agency [30], and consist of the maximum average daily temperature and the relative humidity per each month of the year in Granada (Spain). Fig. 7 depicts the gross and net power, water requirements and energy and exergy efficiency.

Regarding power production, it can be seen that both, gross and net power, are higher for the wet configuration, followed by the hybrid and dry systems. This is mainly due to the ability of the cooling tower to achieve lower condensation pressures. The percentage variation between gross and net power in each case studied is 1.4% for the wet system, 7.2% in the hybrid system and 7.1% in the dry system. As mentioned before, this is because of the high consumption required by the auxiliary equipment, and specifically by the fan of the dry system and the additional pressure loss induced by the evaporative pad in the hybrid system.

It can be mentioned that the power produced by the dry and hybrid systems is closer in the coolest month of the year. As can be seen in Table 5, when the ambient temperature decreases, the relative humidity rises. This fact limits the quantity of water evaporated reducing the latent heat rejected. The effects are an increment of the condensation pressure and, hence, a lower efficiency in the cycle. Furthermore, the dry system can reach lower pressures of condensation in these periods because of the low ambient temperatures.

The energy efficiency of the power plant in each case of study follows the same trend than the power production. It decreases in the warmer months since the temperature of condensation rises and, hence, the pressure, generating less power. The configuration with a higher performance is the wet system, followed by the hybrid and dry systems. The average difference in percentage along the year is 10.70% in the case of the cooling tower and 3.18% in the hybrid system with respect of the dry system.

Regarding the exergetic efficiency of the cycle, it can be observed that the dry system has a better response than the hybrid in July. This is due to the low relative humidity, that causes an increment of the water required and a major inlet exergy in comparison with the exergy generated, decreasing the efficiency.

With respect to the water consumption, the cooling tower consumes a major quantity of water than the hybrid system. The average of the percentage difference along the year is 70.07%, reaching 80% in January, November and December. This fact could be explained due to the high relative humidity in these months that reduces the evaporated water required in the cooling process of the hybrid system since the air reaches a saturated state earlier. As previously mentioned in this section, ambient conditions play an important role in the power plant. The quantity of water required in each month depends on the relative humidity. In winter season the relative humidity increases, reducing the amount of water evaporated and, hence, the latent heat exchange in comparison with summer time as can be seen in Fig. 7. The reduction in water usage by means of hybrid system also involves a decrease of 6.70% in net power production with regard to cooling tower. This fact shows an advantage in the use of hybrid systems in locations where the water scarce exists by reducing power production penalty as it occurred when using dry coolers.

Fig. 8 shows the annual energy production and water usage of the three cases of study, taking into account a heat storage in the power plant that permits a nominal power production during 7.5 h per day. As can be seen, the gross power is 4.3% higher in wet configuration and 3.4% in hybrid than the dry system. In the case of net power, wet and hybrid systems produce a 10.7% and 3.3% more power respectively than the dry system. This difference is mainly because of the summer season penalty, that reduces the power production with regard to the rest of the year. It can also be observed that, by using an hybrid condenser instead of a cooling tower, the water required can be reduced to a 68.4%. This fact shows that there is a huge potential for water saving that can be crucial in zones with water scarcity.

4. Conclusions

This paper presents a comparison between different condensation systems of a solar thermal power plant. The key findings and conclusions may be listed as follows:

- The cycle refrigerated with a cooling tower achieves a lower pressure of condensation, followed by the hybrid and dry system. As the pressure decreases, the efficiency of the cycle increases and also the power generated, being 12.60% in the case of cooling tower and 4.65% in the hybrid system with respect the dry condenser.
- Hybrid and dry configurations require four times major power consumption due to the auxiliary elements of the cooling system, due to it is necessary a high air mass flow in order to dissipate the heat of the condenser. Moreover, hybrid system presents an additional power consumption to overcome the pressure loss of the adiabatic fill. Nevertheless the increment of power consumption produced using this technology compensate the losses.
- Both, cycle and power plant efficiencies are higher using the cooling tower configuration, followed by the hybrid and dry system.
- The wet cooling system requires three times more water than the hybrid system, due to mainly the evaporation process and, to a lesser extent, drift and purges.

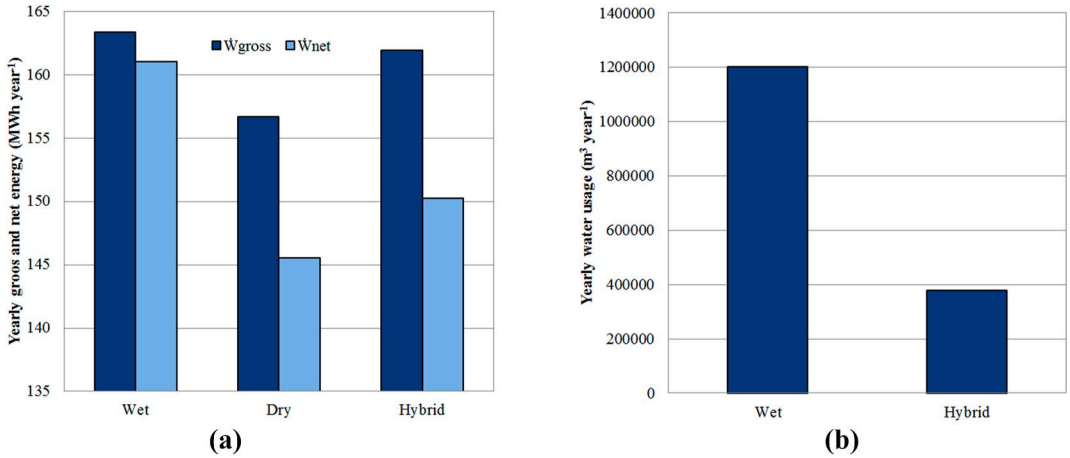

Fig. 8. Annual energy production and water usage.

- A 71.74% of water usage savings by the hybrid system carries a reduction of 7.06% of net power production with regard of the cooling tower configuration
- The dry air condenser is the system with a major rate of exergy destruction (34.66%), followed by the air condenser with adiabatic pre-cooling (33.14%) and the cooling tower (22.28%).

On the whole, the use of hybrid systems, whether as studied in this paper, or in cooling tower and dry system configurations operating in parallel, appears as one of the compromise solutions that will reduce water consumption in the next generation of CSP power plants.

Author statement

C.G. Cutillas: Methodology, Formal analysis, Validation, Writing - Original Draft, Writing - Review & Editing.
J. Ruiz: Methodology, Formal analysis, Writing - Original Draft, Writing - Review & Editing.
F. Asfand: Writing - Review & Editing.
K. Patchigolla: Writing - Review & Editing.
M. Lucas: Conceptualization, Writing - Original Draft, Writing - Review & Editing, Supervision, Funding acquisition.

Declaration of competing interest

The authors declare that they have no known competing financial interests or personal relationships that could have appeared to influence the work reported in this paper.

Acknowledgements

This research is funded by FEDER/Ministerio de Ciencia e Innovación – Agencia Estatal de Investigación, Spain through Spanish research projects ENE2017-83729-C3-1-R and ENE2017-83729-C3-3-R, supplied by FEDER funds.

Appendix A. Cooling pad selection criteria

The selection of a particular cooling pad for a specific application, is not straightforward. A cooling pad with large specific surface area, provides a high cooling efficiency. However, it usually induces a higher pressure drop into the air stream. Hence, the overall performance of a wet cooling pad must be a trade-off between its cooling efficiency and the induced pressure drop. No general rules have been found in the literature in that regard. Some authors have provided general guidelines to accomplish this goal. For example [14], derived a dimensionless parameter, termed as benefit efficiency, that takes into account both cooling efficiency and pressure drop.

An unequivocal criterion for cooling pad selection can be based on the overall energetic performance of the specific application. In this study, CELdek evaporative cooling pads models 5090-15 and 7090-15 were included in the simulations. Four pad thicknesses for each type, adding up to eight cases ranging from 50 to 300 mm, were considered. The performance in terms of cooling efficiency and pressure drop was obtained from the technical sheets provided by the manufacturer. In order to include the geometrical properties of each pad in the hybrid condenser of the solar power plant, it was necessary to calculate the constants α, β and k from equations (22) and (23) according to the technical data. To carry out this task, an optimisation tool to minimise the error was used. As a result, each

constant was defined by a correlated polynomial equation that depends on the thickness of the pad $\alpha = \alpha(\delta)$, $\beta = \beta(\delta)$ and $k = k(\delta)$.

$$\begin{aligned} \alpha &= y_1\delta^3 + y_2\delta^2 + y_3\delta + y_4 \\ \beta &= y_1'\delta^3 + y_2'\delta^2 + y_3'\delta + y_4' \\ k &= y_1''\delta^3 + y_2''\delta^2 + y_3''\delta + y_4'' \end{aligned} \tag{A.1}$$

Hence, the equations of efficiency and pressure drop are modified as:

$$\epsilon = 1 - e^{\left(-\frac{\left(y_1'\delta^3 + y_2'\delta^2 + y_3'\delta + y_4'\right)\delta}{V\left(y_1\delta^3 + y_2\delta^2 + y_3\delta + y_4\right)}\right)} \tag{A.2}$$

$$\Delta p = \left(y_1''\delta^3 + y_2''\delta^2 + y_3''\delta + y_4''\right)V^2 \tag{A.3}$$

The constants for each configuration and equation can be found in Table 6.

Table 6
Constants for Eqs. (A.2) and (A.3).

Pad	y_1	y_2	y_3	y_4	y_1'	y_2'	y_3'	y_4'	y_1''	y_2''	y_3''	y_4''
	[m^{-3}]	[m^{-2}]	[m^{-1}]	[–]	[$m^{-4}\cdot s^{-1}$]	[$m^{-3}\cdot s^{-1}$]	[$m^{-2}\cdot s^{-1}$]	[$m^{-1}\cdot s^{-1}$]	[$Pa\cdot s^{-2}\cdot m^{-5}$]	[$Pa\cdot s^{-2}\cdot m^{-4}$]	[$Pa\cdot s^{-2}\cdot m^{-3}$]	[$Pa\cdot s^{-2}\cdot m^{-2}$]
5090–15	80.000	−26.000	3.100	0.140	2253.538	−474.887	27.501	22.899	9112.660	−2657.285	413.428	−6.224
7090–15	40.000	−30.000	6.000	−0.060	583.389	−403.369	66.454	11.374	−513.223	248.975	51.784	1.633

Fig. 9 presents the influence of the pad in the air-cooled condenser with a wetted-media evaporative pre-cooling. The comparison between gross power, net power and water consumption for the eight cases previously mentioned is shown. These results are also presented in Table 7.

Concerning the pad thickness, the general observed trend for the gross power is that $\uparrow \delta \longrightarrow \uparrow \dot{W}_{gross}$. This is due to the reduced condensing pressure obtained by the pad's increased efficiency (larger exchange area). As an increase in the pad thickness also yields to an increased fan consumption through increased pressure drop, $\uparrow \delta \rightarrow \uparrow \Delta p$, an optimum δ value can be obtained for each pad type concerning net power. This value is $\delta = 0.15$ m for the 5090 type and $\delta = 0.2$ m for the 7090 type.

The performance of the system is also influenced by the pad type. Both types offer similar performance in terms of net power for the same pad thickness. Furthermore, the 5090-type pad uses more water than the 7090. This fact is because of the different geometry of the pads.

In the light of these results, the best pad for this application is the 7090 model with a pad thickness of 200 mm.

These results highlight the importance of the pad selection procedure in hybrid cooling systems. If the pad is not carefully chosen, the net power can be reduced by 0.61%. Besides, the variation in water consumption can reach a difference of 39.46%, from 0.62 to 0.87 m^3/h per MW.

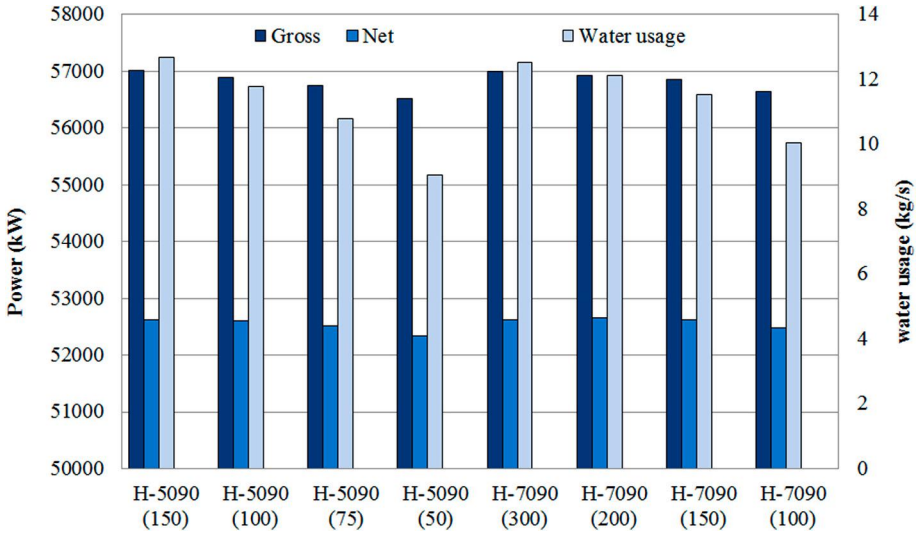

Fig. 9. Evaporative pad comparative in the hybrid configuration.

Table 7
Evaporative pad analysis results.

	5090–15				7090–15			
Thickness	$\delta = 0.15$ m	$\delta = 0.1$ m	$\delta = 0.075$ m	$\delta = 0.05$ m	$\delta = 0.3$ m	$\delta = 0.2$ m	$\delta = 0.15$ m	$\delta = 0.1$ m
Gross power (kW)	57012.93	56887.96	56753.98	56514.94	56991.68	56935.94	56853.74	56652.03
Net power (kW)	52630.93	52612.73	52525.36	52341.96	52621.80	52658.70	52630.22	52481.11
Fan consumption (kW)	4382.00	4275.24	4228.62	4172.99	4369.88	4277.25	4223.52	4170.91
Energy efficiency (−)	0.390	0.389	0.388	0.387	0.390	0.390	0.389	0.388
Condenser exergy destroyed (kW)	7751.37	7665.97	7632.27	7573.92	7743.51	7660.84	7618.53	7577.45
Total exergy destroyed (kW)	23146.95	23165.15	23252.53	23435.96	23156.08	23119.18	23147.66	23296.78
Exergy efficiency (−)	0.691	0.692	0.692	0.693	0.691	0.692	0.693	0.693
Water consumption (kg s^{-1})	12.68	11.77	10.79	9.04	12.52	12.12	11.52	10.05
Water consumption ($m^3h^{-1}MW^{-1}$)	0.867	0.805	0.740	0.622	0.857	0.828	0.788	0.689

References

[1] REE, Red eléctrica de españa. Spanish electricity system 2018 report. https://www.ree.es/sites/default/files/11_PUBLICACIONES/Documentos/InformesSistemaElectrico/2019/Avance_ISE_2018.pdf, 2018.
[2] EPRI, Comparison of Alternate Cooling Technologies for california Power Plants: Economic, environmental, and other tradeoffs, 2002.
[3] A. Cooperman, J. Dieckmann, J. Brodrick, Power plant water use, ASHRAE J. 54 (2012) 65–68.
[4] A. Poullikkas, I. Hadjipaschalis, G. Kourtis, A comparative overview of wet and dry cooling systems for rankine cycle based csp plants, Trends Heat Mass Tran. 13 (2013) 27–50.
[5] A.M. Blanco-Marigorta, M.V. Sanchez-Henríquez, J.A. Peña-Quintana, Exergetic comparison of two different cooling technologies for the power cycle of a thermal power plant, Energy 36 (2011) 1966–1972. URL: http://www.sciencedirect.com/science/article/pii/S0360544210005128, 5th Dubrovnik Conference on Sustainable Development of Energy, Water & Environment Systems.
[6] M. Gupta, S. Kaushik, Exergy analysis and investigation for various feed water heaters of direct steam generation solar–thermal power plant, Renew. Energy 35 (2010) 1228–1235. URL: http://www.sciencedirect.com/science/article/pii/S0960148109004029.
[7] A.M. Patnode, Simulation and Performance Evaluation of Parabolic Trough Solar Power Plants, Ph.D. thesis, University of Wisconsin-Madison, 2006.
[8] T.K. Aseri, C. Sharma, T.C. Kandpal, Estimation of capital costs and techno-economic appraisal of parabolic trough solar collector and solar power tower based csp plants in India for different condenser cooling options, Renew. Energy 178 (2021) 344–362, https://doi.org/10.1016/j.renene.2021.05.166. URL: https://www.sciencedirect.com/science/article/pii/S0960148121008557.
[9] K. Hooman, Z. Guan, H. Gurgenci, 9 - advances in dry cooling for concentrating solar thermal (cst) power plants, in: M.J. Blanco, L.R. Santigosa (Eds.), Advances in Concentrating Solar Thermal Research and Technology, Woodhead Publishing Series in Energy, Woodhead Publishing, 2017, pp. 179–212. URL: http://www.sciencedirect.com/science/article/pii/B9780081005163000095.
[10] M.J. Wagner, C.F. Kutscher, Assessing the Impact of Heat Rejection Technology on Csp Plant Revenue, 2010.
[11] E. Rezaei, S. Shafiei, A. Abdollahnezhad, Reducing water consumption of an industrial plant cooling unit using hybrid cooling tower, Energy Convers. Manag. 51 (2010) 311–319. URL: https://www.sciencedirect.com/science/article/pii/S0196890409003811.
[12] A. Ashwood, D. Bharathan, Hybrid Cooling Systems for Low-Temperature Geothermal Power Production, 2011.
[13] T. Tang, J. qun Xu, S. xiang Jin, H. qi Wei, Study on operating characteristics of power plant with dry and wet cooling systems, Energy Power Eng. 5 (2013) 651–656. URL: https://www.scirp.org/journal/PaperInforCitation.aspx?PaperID=38813.
[14] S. He, H. Gurgenci, Z. Guan, X. Huang, M. Lucas, A review of wetted media with potential application in the pre-cooling of natural draft dry cooling towers, Renew. Sustain. Energy Rev. 44 (2015) 407–422. URL: http://www.sciencedirect.com/science/article/pii/S1364032114010892.
[15] S. He, H. Gurgenci, Z. Guan, K. Hooman, Z. Zou, F. Sun, Comparative study on the performance of natural draft dry, pre-cooled and wet cooling towers, Appl. Therm. Eng. 99 (2016) 103–113. URL: https://www.sciencedirect.com/science/article/pii/S1359431116300102.
[16] J.G. Bustamante, A.S. Rattner, S. Garimella, Achieving near-water-cooled power plant performance with air-cooled condensers, Appl. Therm. Eng. 105 (2016) 362–371. URL: https://www.sciencedirect.com/science/article/pii/S1359431115005219.
[17] F. Asfand, P. Palenzuela, L. Roca, A. Caron, C.-A. Lemarié, J. Gillard, P. Turner, K. Patchigolla, Thermodynamic performance and water consumption of hybrid cooling system configurations for concentrated solar power plants, Sustainability 12 (2020) 1–19. URL: https://www.mdpi.com/2071-1050/12/11/4739.
[18] A. Alkhedhair, H. Gurgenci, I. Jahn, Z. Guan, S. He, Numerical simulation of water spray for pre-cooling of inlet air in natural draft dry cooling towers, Appl. Therm. Eng. 61 (2013) 416–424. URL: http://www.sciencedirect.com/science/article/pii/S135943111300584X.
[19] M. Lucas, P. Martínez, C.G. Cutillas, P.J. Martínez, J. Ruiz, A.S. Kaiser, B. Zamora, Experimental optimization of the thermal performance of a dry and adiabatic fluid cooler, Appl. Therm. Eng. 69 (2014) 1. – 10. URL: http://www.sciencedirect.com/science/article/pii/S135943111400297X.
[20] M.J. Moran, 6 - availability and chemical availability, in: K. Wagstaff (Ed.), Availability Analysis: A Guide to Efficient Energy Use, Prentice-Hall, Inc., 1982, pp. 122–145.
[21] D. Meng, Q. Liu, Z. Ji, Performance analyses of regenerative organic flash cycles for geothermal power generation, Energy Convers. Manag. 224 (2020) 113396, https://doi.org/10.1016/j.enconman.2020.113396. URL: https://www.sciencedirect.com/science/article/pii/S0196890420309328.
[22] M. Poppe, H. Rögener, Berechnung von rückkühlwerken, VDI wärmeatlas, 1991. Mi 1.
[23] J. Kloppers, D. Kröger, Cooling tower performance evaluation: Merkel, poppe, and e–ntu methods of analysis, J. Eng. Gas Turbines Power-Trans. Asme - J. Eng. Gas Turb Power-T ASME 127 (2005).
[24] J. Ruiz, A. Kaiser, M. Lucas, Experimental determination of drift and pm_{10} cooling tower emissions: influence of components and operating conditions, Environ. Pollut. 230 (2017) 422–431, https://doi.org/10.1016/j.envpol.2017.06.073. URL: https://www.sciencedirect.com/science/article/pii/S026974911731120X.
[25] J. Wu, X. Huang, H. Zhang, Theoretical analysis on heat and mass transfer in a direct evaporative cooler, Appl. Therm. Eng. 29 (2009) 980–984. URL: http://www.sciencedirect.com/science/article/pii/S1359431108002275.
[26] S. He, H. Gurgenci, Z. Guan, A.M. Alkhedhair, Pre-cooling with munters media to improve the performance of natural draft dry cooling towers, Appl. Therm. Eng. 53 (2013) 67–77. URL: http://www.sciencedirect.com/science/article/pii/S1359431113000070.
[27] P. Martínez, J. Ruiz, P. Martínez, A. Kaiser, M. Lucas, Experimental study of the energy and exergy performance of a plastic mesh evaporative pad used in air conditioning applications, Appl. Therm. Eng. 138 (2018) 675–685. URL: http://www.sciencedirect.com/science/article/pii/S1359431117378225.
[28] Q. Liu, L. Shang, Y. Duan, Performance analyses of a hybrid geothermal–fossil power generation system using low-enthalpy geothermal resources, Appl. Energy 162 (2016) 149–162, https://doi.org/10.1016/j.apenergy.2015.10.078. URL: https://www.sciencedirect.com/science/article/pii/S0306261915013057.
[29] P. Puckorius, Why evaporative coolers have not caused legionnaires' disease, ASHRAE J. (1995) 29–33.
[30] AEMET, Agencia estatal de meteorología. guía resumida del clima en españa, URL: http://www.aemet.es/es/serviciosclimaticos/datosclimatologicos/valoresclimatologicos?l=5530E&k=and, 2012.